Dieses Manuskript wurde im Tagungsband der ITG/GMA-Fachtagung „Sensoren und Messsysteme 2006“ veröffentlicht, welcher im VDE Verlag GmbH erschienen ist. Die Arbeit wurde am 13.03.2006 mit dem „Best Paper Award“ des deutschen IEEE Instrumentation and Measurement (I&M) Chapter ausgezeichnet.


IM Chapter IEEE Germany Section

http://smarthome.unibw-muenchen.de/IMC/

BEST PAPER AWARD

Name(s): A. Mellinger[1], R. Suárez[1], R. Singh[2], M. Wegener[1] W. Wirges[1], S. Lang[3], R. Gerhard-Multhaupt[1]

Organisation: [1] University of Potsdam, Germany; [2] University of Allahabad, India; [3] Ben-Gurion University of the Negev, Israel

For the Outstanding Paper: High-resolution Space-Charge and Polarization Tomography with Thermal Pulses

Freiburg, March 13-14, 2006

Dr.-Ing. Olfa Kanoun
Chapter Chair

IEEE IEEE IEEE IEEE IEEE IEEE IEEE IEEE IEEE

High-resolution Space-Charge and Polarization Tomography with Thermal Pulses

Priv.-Doz. Dr. Axel Mellinger[1], M. Sc. Rosaura Flores Suárez[1], M. Sc. Rajeev Singh[2], Dr. Michael Wegener[1], Dipl.-Ing. Werner Wirges[1], Prof. Dr. Sidney B. Lang[3], Prof. Dr. Reimund Gerhard-Multhaupt[1]
[1] *Universität Potsdam, Institut für Physik, Am Neuen Palais 10, 14469 Potsdam, Germany*
[2] *Department of Electronics & Communication, University of Allahabad, Allahabad, (U.P.)-211002, India*
[3] *Department of Chemical Engineering, Ben-Gurion University of the Negev, P.O.B. 653, 84105 Beer Sheva, Israel*

Abstract

Three-dimensional imaging of space-charge and polarization distributions in electret materials has been implemented by means of laser-induced thermal pulses. In pyroelectric films of poled poly(vinylidene fluoride), images of 45×45 pixels with a depth-resolution of less than 0.5 µm and a lateral resolution of 40 µm were recorded, the latter being limited by fast thermal diffusion in the absorbing front electrode. Initial applications include the analysis of polarization distributions in corona-poled piezoelectric sensor cables and the detection of patterned space-charge distributions in polytetrafluoroethylene films.

1 Introduction

The non-destructive detection of polarization and space-charge distributions in the crystalline and amorphous phase of polymers is of prime importance in electret research and the development of transducer materials. Since the 1970s, a number of techniques for probing the depth profile of the internal electric field have been developed. They all share the basic concept of using an external stimulus (usually optical, thermal, mechanical, or electrical) to generate local, temperature- or pressure-induced changes in the geometry or permittivity of the sample (see the example shown in Fig. 1), thus giving rise to a response (electrical or mechanical) that carries information on the spatial distribution of embedded electric dipoles or space charges. Compared to their acoustic counterparts, thermal depth-profiling techniques have the advantage of providing sub-µm near-surface resolution at moderate cost [1]. Additionally, when the stimulus is provided via the absorption of light by an opaque front electrode, this method can be applied *in situ* for, e. g., experiments in a vacuum environment.

Thermal profiling has been implemented both in the frequency domain (commonly referred to as the laser intensity modulation method, LIMM [2]), and in the time domain (thermal pulse (TP) technique) [3]. A recent comparison of LIMM and TP showed excellent agreement between the two techniques (Fig. 2). However, the thermal-pulse measurements could be carried out up to 50 times faster than a comparable LIMM scan. This high data acquisition speed made it possible to implement a tomographic setup where the samples are scanned with a focused laser beam. Similar setups implemented in the frequency domain face a trade-off between a higher depth resolution with a limited number of beam pointings [4] or a high-resolution X-Y map with limited depth-information [5, 6].

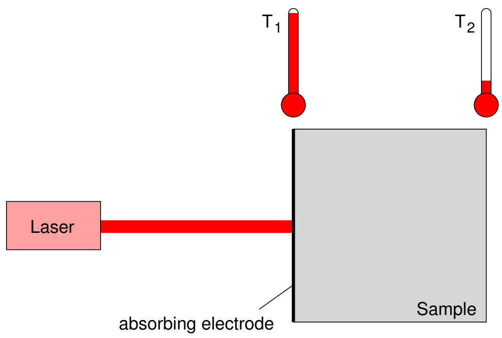

Figure 1: Principle of the thermal-pulse method. The absorbed laser beam gives rise to a spatially modulated temperature distribution.

2 Experimental Setup

The experimental setup for planar samples is shown in Fig. 3. Thermal pulses were generated by means of a Q-switched, frequency-doubled Nd:YAG laser (Polaris III, New Wave Research) operating at repetition rates of 2. . . 6 Hz (imposed by the speed of the data acquisition system). The samples (typically, polymer films of 10. . . 250 µm thickness) were coated on both sides with non-transparent 200 nm aluminum or copper electrodes in high vacuum and glued to a stainless steel substrate in order to avoid thermo-elastic resonances [7]. Sample positioning in the laser beam was carried out with an X-Y motorized translation stage (ERLIC 85, OWIS GmbH) and a manual Z translation stage. By varying the Z position along the optical axis, the $1/e^2$ beam spot size could be adjusted between 30 and 400 µm [8]. By adding a rotary stage, piezoelectric polymer cables made from P(VDF-TrFE) (the copolymer of vinylidene fluoride with trifluoroethylene), could be investigated as well (cf. Fig. 4). The core wires of the coaxial cables (Huber & Suhner, Switzerland) were removed and replaced by a stainless steel pin of 0.7 mm diameter.

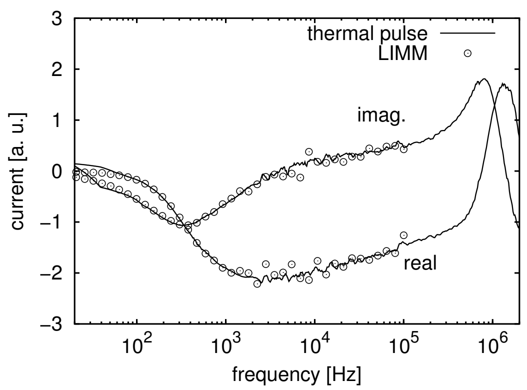

Figure 2: Comparison of the Fourier-transformed thermal-pulse signal (solid line) and the LIMM spectrum (open circles) of a volume-charged polytetrafluoroethylene (PTFE) film of 17 µm thickness. Data acquisition time was 40 s for the TP signal vs. 30 min for the LIMM curve. (From [9].)

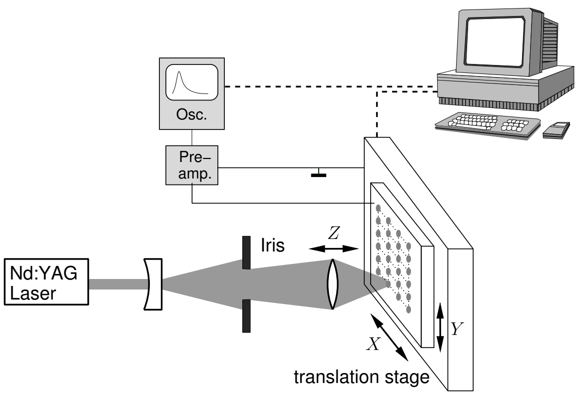

Figure 3: Experimental setup for focused thermal-pulse tomography.

A 200 nm Cu layer evaporated onto the P(VDF-TrFE) insulator served as outer electrode.

The short-circuit current was amplified by a Stanford Research SR 570 current-to-voltage converter and recorded with a digital storage oscilloscope (Agilent 54833A). To improve the signal-to-noise ratio, 30 to 50 pulses were averaged for each beam pointing. As each transient has approx. $N = 512\,000$ data points, the total amount of raw data for a 2 kPixel pyroelectric image is of the order of 4 GB.

3 Data Processing

The transient thermal-pulse current $I(t_k)$, $k = 1 \ldots N$, was Fourier-transformed [10] into the frequency domain and corrected for the frequency-dependent preamplifier gain and phase-shift $\tilde{\alpha}(f_n)$ [9]:

$$\tilde{J}_{\exp}(f_n) = \frac{\Delta t}{\tilde{\alpha}(f_n)} \sum_{k=0}^{N-1} I(t_k) e^{-2\pi i k n/N}\,, \qquad (1)$$

with

$$f_n = \frac{n}{N\Delta t}\,, \qquad n = 1 \ldots \frac{N}{2}\,, \qquad (2)$$

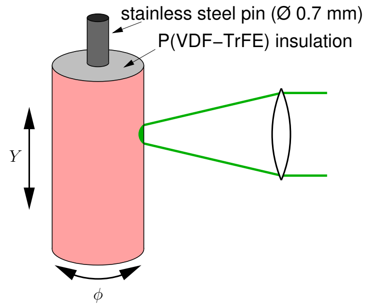

Figure 4: Focused thermal-pulse method applied to piezoelectric coaxial sensor cables.

where Δt is the sampling interval. The relation between the profile of the pyroelectric coefficient $p(x,y,z)$ and the pyroelectric current is given by the LIMM equation

$$\tilde{J}(f_n) = \frac{i2\pi f_n}{d} \int_0^d \int_{-\infty}^{\infty} \int_{-\infty}^{\infty} p(x,y,z) \quad \times \\ \times \quad \tilde{T}(x,y,z,f_n)\,\mathrm{d}x\,\mathrm{d}y\,\mathrm{d}z\,, \qquad (3)$$

where d is the sample thickness and $\tilde{T}(x,y,z,f_n)$ is the frequency-domain temperature amplitude of the thermal wave. In the 1-dimensional approximation, Eq. (3) reduces to [11]:

$$\tilde{J}(f_n) = \frac{i2\pi f_n A}{d} \int_0^d p(z)\tilde{T}(z,f_n)\,dz\,, \qquad (4)$$

where the (complex) temperature distribution $\tilde{T}(z,f_n)$ is given by the solution of the one-dimensional heat conduction equation [7, 12].

Mathematically, Eqs. (3) and (4) are known as a Fredholm integral equation of the first kind, the solution of which is an ill-posed problem. Several techniques have been used in order to extract physically meaningful solutions $p(z)$ from one-dimensional experimental data, such as Tikhonov regularization [13], iterative schemes [14] or a scale-transformation method [15]. Here, either a polynomial regularization approach [11] or the scale-transformation method were used for reconstructing the pyroelectric distribution. A general solution for the inversion of the three-dimensional LIMM equation (3) is currently under development.

4 Results and Discussion

4.1 Planar Poly(vinylidene fluoride) Films

The polarization map of an 11 µm uniaxially stretched β-poly(vinylidene fluoride) (PVDF) film poled with a 'T'-shaped upper aluminum electrode (later covered by a light-absorbing 200 nm Cu electrode) is shown in Fig. 5. The image covers an area of 7×7 mm^2 scanned with a step size of 200 µm. The structure of the original 'T' electrode is very well revealed. Even

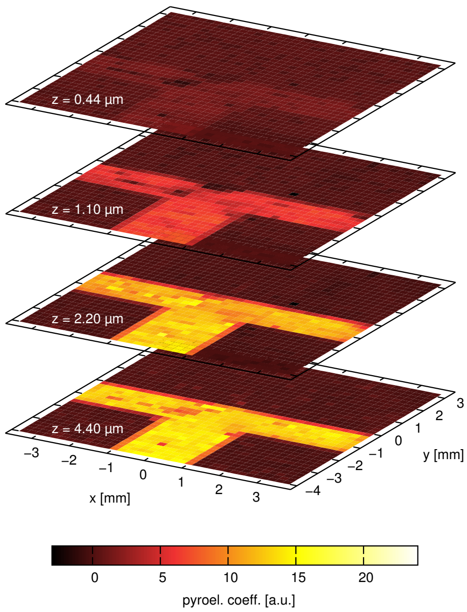

Figure 5: Polarization map of an 11 µm PVDF film poled with a patterned electrode.

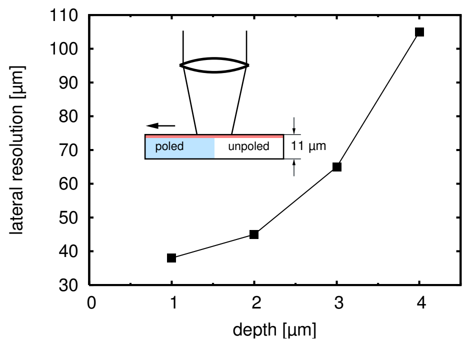

Figure 6: Depth-dependence of the lateral resolution in PVDF (same sample as in Fig. 5) at a beam spot size of 30 µm. The data was obtained by scanning the poled/unpoled transition region, as shown in the inset.

though the poling field was twice the coercive field of 50 V/µm, the polarization maps at different depths reveal a substantial edge depolarization that probably results from surface impurities. As evident from Fig. 5, the depth-resolution was better than 0.5 µm. The lateral resolution of the tomographic technique was tested by performing 1-dimensional scans across the edge of the 'T' electrode in the Y direction [16] at the tightest spot size of 30 µm. As shown in Fig. 6, the lateral resolution increases from 38 µm at a depth of 1 µm to over 100 µm at a depth of 4 µm. This represents a significant improvement over recent 3-dimensional acoustic measurements [17]. The depth-dependence of the lateral resolution is caused by the very different thermal diffusivities $D = \kappa/(c\rho)$ of the electrode and the polymer material (where κ denotes the thermal conductivity and $c\rho$ the volumetric heat capacity). As the diffusion length at a given time t is $\ell = \sqrt{Dt}$, the thermal pulse exhibits a lateral diffusion speed in the electrode (with a diffusivity of approx. 10^{-4} m^2/s) some 30× faster than the vertical diffusion into the polymer (where $D \approx 10^{-7}$ m^2/s). As a consequence, the heated front electrode cools down more rapidly than the polymer, thus turning from a heat source to a heat sink. Recent finite-element calculations of the temporal and spatial evolution of the heat pulse confirmed this qualitative discussion [8]. Improving the lateral resolution will require a surface electrode with a good electrical conductivity, but low thermal diffusivity.

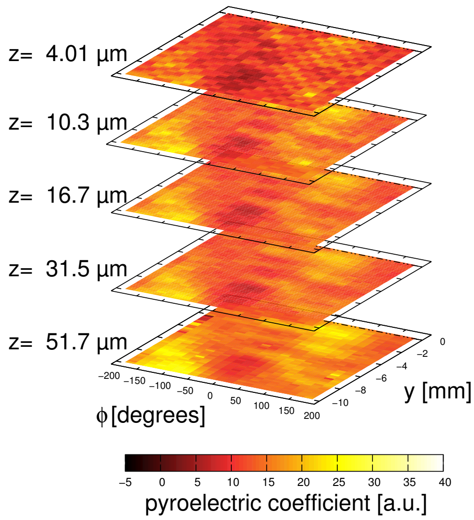

Figure 7: Polarization map of a piezoelectric sensor cable poled in a continuous process with 4 corona needles at +20 kV.

4.2 PVDF-TrFE Coaxial Sensor Cables

Coaxial sensor cables (where the active layer consists of piezoelectric PVDF-TrFE) have found important applications in traffic monitoring and intrusion detection. Typically, they are poled (and thus given their piezoelectric properties) by subjecting the extruded cables to a corona discharge formed by a series of high-voltage points around the cable. While their overall piezoelectric properties have been well-studied [18], little was known about the spatial distribution of the polarization. In the present study, polarization maps were obtained from cables poled either in the above-described continuous process or in the laboratory with a single needle. As evident in Fig. 7, the former show a rather uneven distribution that can be attributed to the fact that any point on the cable was exposed to the corona discharge for no more than 300 ms at the given extrusion speed. The laboratory-poled cable, on the other hand, show a smooth polarization centered on the needle position (Fig. 8).

4.3 Space-Charge Electrets

The focused thermal-pulse method is also capable of detecting space-charge distributions in non-polar materials. As an example, films of polytetrafluoroethylene

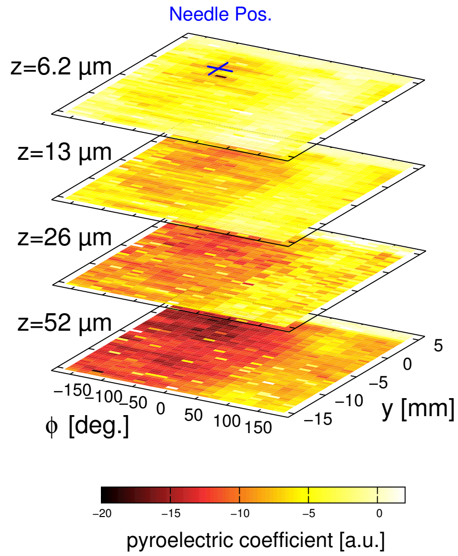

Figure 8: Polarization map of a piezoelectric sensor cable poled for 30 s with a single fixed needle at −25 kV. The cross marks the projected needle position.

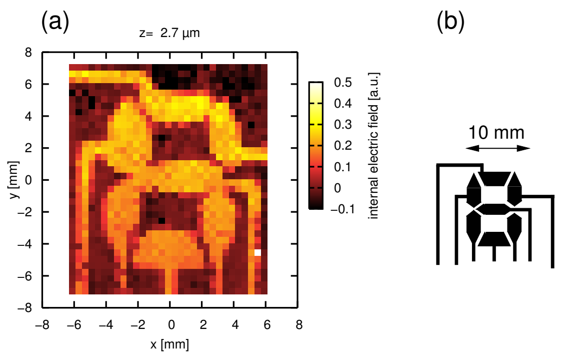

Figure 9: Internal electric field in electron-beam irradiated PTFE film ($d = 17$ µm): (a) field distribution at a depth of $z = 2.7$ µm, (b): shadow mask used for charging. (From [8].)

(PTFE, thickness 17 µm) were irradiated with a monoenergetic electron beam (15 keV) through a shadow mask (cf. Fig. 9b). The resulting patterned space-charge distribution could be imaged with the focused TP method, as shown in Fig. 9a. All details of the mask are very well reproduced by the space-charge pattern.

5 Conclusions

The focused thermal-pulse technique is a versatile, non-destructive method for obtaining tomographic images of space-charge and polarization distributions. A depth-dependent lateral resolution of between 38 and 105 µm have been demonstrated in PVDF films. As demonstrated in piezoelectric PVDF-TrFE sensor cables, the method is suitable for controlling and optimizing the poling process. Work is in progress to improve the lateral resolution by optimizing the electrode material with respect to conductivity and thermal diffusivity, as well through a numerical data-analysis procedure that takes into account the in-plane thermal diffusion.

Acknowledgment

The authors would like to thank Lucas F. Santos (Instituto de Física de São Carlos, Brazil) for providing the electron-beam charged PTFE samples.

References

[1] S. Bauer and S. Bauer-Gogonea, *Current practice in space charge and polarization profile measurements using thermal techniques*. IEEE Trans. Dielectr. Electr. Insul. **10**, 883–902 (2003).

[2] S. B. Lang and D. K. Das-Gupta, *A technique for determining the polarization distribution in thin polymer electrets using periodic heating*. Ferroelectrics **39**, 1249–1252 (1981).

[3] R. E. Collins, *Analysis of spatial distribution of charges and dipoles in electrets by a transient heating technique*. J. Appl. Phys. **47**, 4804–4808 (1976).

[4] D. Marty-Dessus, L. Berquez, A. Petre and J. L. Franceschi, *Space charge cartography by FLIMM: a three-dimensional approach*. J. Phys. D: Appl. Phys. **35**, 3249–3256 (2002).

[5] B. Ploss, W. Hassler, H. Hulz and G. Kobernik, *Investigation of the polarization depth distribution of PZT thick films by LIMM*. In: *Proc. 11th IEEE Symp. on Applications of Ferroelectrics*, pp. 207–210, IEEE Service Center, Piscataway, NJ (1998).

[6] A. Quintel, J. Hulliger and M. Wübbenhorst, *Analysis of the polarization distribution in a polar perhydrotriphenylene inclusion compound by scanning pyroelectric microscopy*. J. Phys. Chem. B **102**, 4277–4283 (1998).

[7] P. Bloß and H. Schäfer, *Investigations of polarization profiles in multilayer systems by using the laser intensity modulation method*. Rev. Sci. Instrum. **65**, 1541–1550 (1994).

[8] A. Mellinger, R. Singh, M. Wegener, W. Wirges, R. Flores Suárez, S. B. Lang, L. F. Santos and R. Gerhard-Multhaupt, *High-resolution three-dimensional space-charge and polarization mapping with thermal pulses*. In: *Proceedings, 12th International Symposium on Electrets*, pp. 212–215, IEEE Service Center, Piscataway, NJ (2005).

[9] A. Mellinger, R. Singh and R. Gerhard-Multhaupt, *Fast thermal-pulse measurements of space charge distributions in electret polymers*. Rev. Sci. Instr. **76**, 013903 (2005).

[10] M. Frigo and S. G. Johnson, *The design and implementation of FFTW3*. Proc. IEEE **93**, 216231 (2005).

[11] S. B. Lang, *Laser intensity modulation method (LIMM): Review of the fundamentals and a new method for data analysis*. IEEE Trans. Dielectr. Electr. Insul. **11**, 3–12 (2004).

[12] B. Ploss, S. Bauer and C. Bon, *Measurement of the thermal diffusivity of thin films with bolometers and with pyroelectric temperature sensors*. Ferroelectrics **118**, 435–450 (1991).

[13] A. N. Tikhonov, A. V. Goncharskii, V. V. Stepanov and I. V. Kochikov, *Ill-posed image processing problems*. Sov. Phys.-Doklady **32**, 456–458 (1987).

[14] A. Mellinger, *Unbiased iterative reconstruction of polarization and space-charge profiles from thermal-wave experiments*. Meas. Sci. Technol. **15**, 1347–1353 (2004).

[15] B. Ploss, R. Emmerich and S. Bauer, *Thermal wave probing of pyroelectric distributions in the surface region of ferroelectric materials: A new method for the analysis*. J. Appl. Phys. **72**, 5363–5370 (1992).

[16] A. Mellinger, R. Singh, M. Wegener, W. Wirges, R. Gerhard-Multhaupt and S. B. Lang, *Three-dimensional mapping of polarization profiles with thermal pulses*. Appl. Phys. Lett. **86**, 082903 (2005).

[17] T. Maeno, *Three-dimensional PEA charge measurement system*. IEEE Trans. Dielectr. El. Insul. **8**, 845–848 (2001).

[18] M. Wegener and R. Gerhard-Multhaupt, *Electric poling and electromechanical characterization of 0.1 mm-thick sensor films and 0.2 mm-thick cable layers from piezoelectric poly(vinylidene fluoride-trifluoroethylene)*. IEEE Trans. Ultrason. Ferroelectr. Freq. Control **50**, 921–931 (2003).